

A New Modeling Method of Photoplethysmography Signal Based on Lognormal Basis

Yun Luo¹, Wenfeng Li^{1(✉)}, Wenbi Rao^{2(✉)}, Xiuwen Fu¹, Lin Yang¹,
and Yu Zhang¹

¹ School of Logistics Engineering, Wuhan University of Technology,
Wuhan, People's Republic of China
504200297@qq.com,

{liwf, XiuwenFu, lyang, sanli}@whut.edu.cn

² School of Computer Science and Technology,
Wuhan University of Technology, Wuhan, People's Republic of China
wbrao@whut.edu.cn

Abstract. Human photoplethysmography (PPG) signal carries abundant physio-logical and pathological information of cardiovascular system, which can be used to monitor cardiovascular health in the daily life. The existing modeling methods are mainly based on Gaussian basis, which fail to conform to the long-tail features of PPG pulse waveforms. And other several existing methods based on Lognormal basis don't work well in daily monitoring. In this paper, we proposed a new modeling method based on the long-tail Lognormal basis. Fitting calculations get an adaptive time domain by introducing the mode of the corresponding Lognormal basis and are implemented by the proposed successive-fitting solution. The simulations have proved that the proposed method has a good fitting accuracy and efficiency and is suitable for daily monitoring of cardiovascular health in body sensor networks (BSNs). Besides that, a closer relation between the cardiovascular health and the vector parameters of the Lognormal basis also can be expected.

Keywords: PPG · Lognormal basis · Modeling · Daily monitoring

1 Introduction

PPG signal contains lots of human physiological and pathological information. Analyzing the PPG signal is an important method to diagnosis cardiovascular health in BSNs [1–3]. Until now, PPG signal has been widely used for monitoring cardiovascular health in the daily life [4–7]. As shown in Fig. 1, a PPG pulse waveform can be divided into two branches and usually contains three waves. The first wave is the main wave. The tidal wave is in the middle of the main wave and the dicrotic notch. The dichotic wave is behind the dicrotic notch. Peaks of the three waves carry rich physiological and pathological information of the cardiovascular system.

PPG pulse waveforms have obvious long-tail features. The existing modeling methods are mainly based on Gaussian basis [8–10], which fail to conform to the

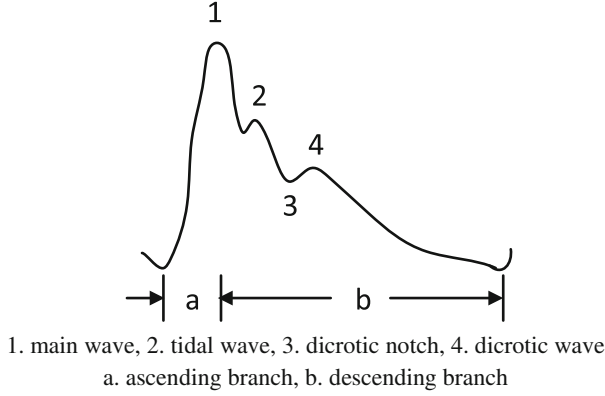


Fig. 1. PPG signal

long-tail features of PPG pulse waveforms. And other several existing methods based on Lognormal basis don't work well in daily monitoring [11–13]. In [8], the researchers used a six Gaussian bases model to fitting the PPG signal, the method has a high fitting accuracy, but the efficiency is not suitable for daily monitoring of cardiovascular health. [9] used a three Gaussian bases model. [10] proposed a successive fitting method to detect the secondary peak, but didn't give a modeling solution for the PPG signal. [11] used a single fitting model with five Lognormal bases, and get a good goodness of fit after iteration process, but the efficiency is not suitable for daily monitoring. [12] used a single fitting model with four Lognormal bases. [13] used a successive fitting model with four Lognormal bases, but the time domain of each fitting calculation is fixed, which can't adjust to different periods of PPG signals independently, so the accuracy is limited and the effect is not very good used in daily monitoring. In this paper, we proposed a successive-fitting solution based on the long-tail Lognormal basis, and introduced the mode of the corresponding Lognormal basis to get an adaptive time domain of the fitting calculations.

The structure of this paper is organized as follows. The background of this paper is briefly introduced in Sect. 1. In Sect. 2, the method of Lognormal basis modeling is depicted. The simulation results are illustrated in Sect. 3. The conclusions are drawn in Sect. 4.

2 Method of Lognormal Basis Modeling

2.1 Physiological Mechanism of PPG Pulse Waveforms

Initial waves are generated in the proximal aorta due to the left ventricular systolic and diastolic activities. Initial waves propagate along the arterial tree and corresponding reflected waves are created by the vascular resistance during the propagation. Therefore, the obtained PPG signal not only carry the information of left ventricular ejection

and the aortic valve closure, but also resistance information (e.g., arterial wall elasticity, peripheral vascular resistance and blood viscosity).

(a) Initial Waves. In the early stage of the left ventricular contraction, the left ventricle squeezes blood into the aorta. At this point, the blood that flows into the proximal aorta is much more than the outflow, which makes intravascular blood volume increases rapidly. As the blood vessel pressure is proportional to the blood volume, the pressure of the blood vessel rises rapidly. The blood vessel wall is under more pressure than normal, so it expands rapidly. In the later stage of the left ventricular contraction, as the left ventricular ejection velocity slows down gradually, the blood that flows into the proximal aorta is less than the outflow, intravascular blood volume and the pressure of the blood vessel gradually decrease, thus making blood vessel wall recoil.

The PPG pulse waveform that caused by the left ventricular contraction is called the main wave. In the diastolic period, the left ventricular pressure is decreasing. This phenomenon would cause the proximal aorta blood flow to the left ventricle. At the meanwhile, blood continues to flow out from the proximal aorta, thus causing the accelerated decrease of the intravascular volume and pressure, and the recoiling of blood vessel wall. After a short time, aortic valve is closed, the blood that flow to the left ventricle would crash against the aortic valve and flow back again to the proximal aorta. At the same time, due to the inertia, the blood that from the adjacent vascular segment continues to flow to the proximal aorta. Two strands of blood promote the brief increase of the proximal aorta's blood volume and pressure, and the expansion of the blood vessel wall. The PPG pulse waveform that caused by the closure of the aortic valve is called the dicrotic wave.

(b) Reflected Waves. After the PPG pulse waveform is formed in the proximal aorta, it propagates along the arterial tree. And reflected waves are generated under the influence of aortic physiological factors (e.g., arterial wall elasticity, peripheral vascular resistance and blood viscosity). This makes a part of blood flow back to the aorta, increasing the intravascular blood volume and the blood vessel pressure, and thus expanding the blood vessel wall. The reflected wave of the main wave is called the tidal wave, and the reflected wave of the dicrotic wave is called the trailing wave.

2.2 Model of PPG Pulse Waveforms

(a) Segmentation of PPG Pulse Waveforms. The main wave of a PPG pulse waveform is created by left ventricular contraction. The tidal wave is the reflected wave of the main wave. The dicrotic notch is caused by the flowing back of the blood to the left ventricle in the proximal aorta. The dicrotic wave is caused by the closure of the aortic valve. And the reflected wave of the dicrotic wave is called the trailing wave. So a PPG pulse waveform is composed by the main wave W_1 , the tidal wave W_2 , the dicrotic wave W_3 and the tail wave W_4 . Assume the start time of W_1, W_2, W_3, W_4 are

t_1, t_2, t_3, t_4 respectively. The start time and end time of PPG signal are t_{str} , t_{end} respectively. Then the fitting PPG signal W can be expressed as:

$$W = \begin{cases} W_1, & t_1 = t_{str}, t_1 \leq t < t_2 \\ W_1 + W_2, & t_2 \leq t < t_3 \\ W_1 + W_2 + W_3, & t_3 \leq t < t_4 \\ W_1 + W_2 + W_3 + W_4, & t_4 \leq t \leq t_{end} \end{cases} \quad (1)$$

The fitting PPG signal can be expressed in the time domain as:

$$W(t) = \begin{cases} W_1(t - t_1), & t_1 = t_{str}, t_1 \leq t < t_2 \\ W_1(t - t_1) + W_2(t - t_2), & t_2 \leq t < t_3 \\ W_1(t - t_1) + W_2(t - t_2) + W_3(t - t_3), & t_3 \leq t < t_4 \\ W_1(t - t_1) + W_2(t - t_2) + W_3(t - t_3) + W_4(t - t_4), & t_4 \leq t \leq t_{end} \end{cases} \quad (2)$$

$t_1 = t_{str} = t_1 < t_2 < t_3 < t_4 < t_{end}$

(b) Lognormal Basis. PPG pulse waveform is characterized as long-tail. To improve the fitting accuracy, here Lognormal basis is used to fit the PPG signal. The finite Lognormal basis $W_i(t)$ is defined as:

$$W_i(t) = \frac{\alpha_i}{t - t_i} \exp\left(\frac{(\ln(t - t_i) - \beta_i)^2}{\gamma_i}\right), \quad \gamma_i < 0, i = 1, 2, 3, 4 \quad (3)$$

Then the Lognormal basis parameters can be defined as $L_i = \{t_i, \alpha_i, \beta_i, \gamma_i\}$. Adding the end time, a PPG pulse waveform's parameters can be expressed as $L = \{t_1, \alpha_1, \beta_1, \gamma_1, t_2, \alpha_2, \beta_2, \gamma_2, t_3, \alpha_3, \beta_3, \gamma_3, t_4, \alpha_4, \beta_4, \gamma_4, t_{end}\}$. Namely a PPG pulse waveform can be represented by a feature vector of 17 parameters.

2.3 Successive-Fitting Solution

The fitting efficiency is determined by the number of the fitting function's parameters. In this paper, we present a solution that uses a successive-fitting with single function instead of a single-fitting with multiple functions. The successive-fitting solution include the main wave fitting, the tidal wave fitting, the dicrotic wave fitting and the tail wave fitting. The whole fitting process is shown in Fig. 2.

(a) Main Wave Fitting. W_D denotes a period of the original PPG signal. The start and end time of W_D are t_{str} and t_{end} . The main peak of W_D is denoted as $t_{p1} \cdot t_{sd1}$ denotes the left zero crossing point around t_{p1} . Considering that the time domain of the existing fitting calculations lacks adaptive adjustment, we introduce M_1 which represents the mode of W_1 . M_1 and its rang are expressed in Eq. (5). The start time of W_1 denoted as t_1 equals the start time of W_D denoted as t_{str} . The optimal Lognormal basis representation is obtained by minimizing the mean squared error (MSE_1) between W_1 and W_D .

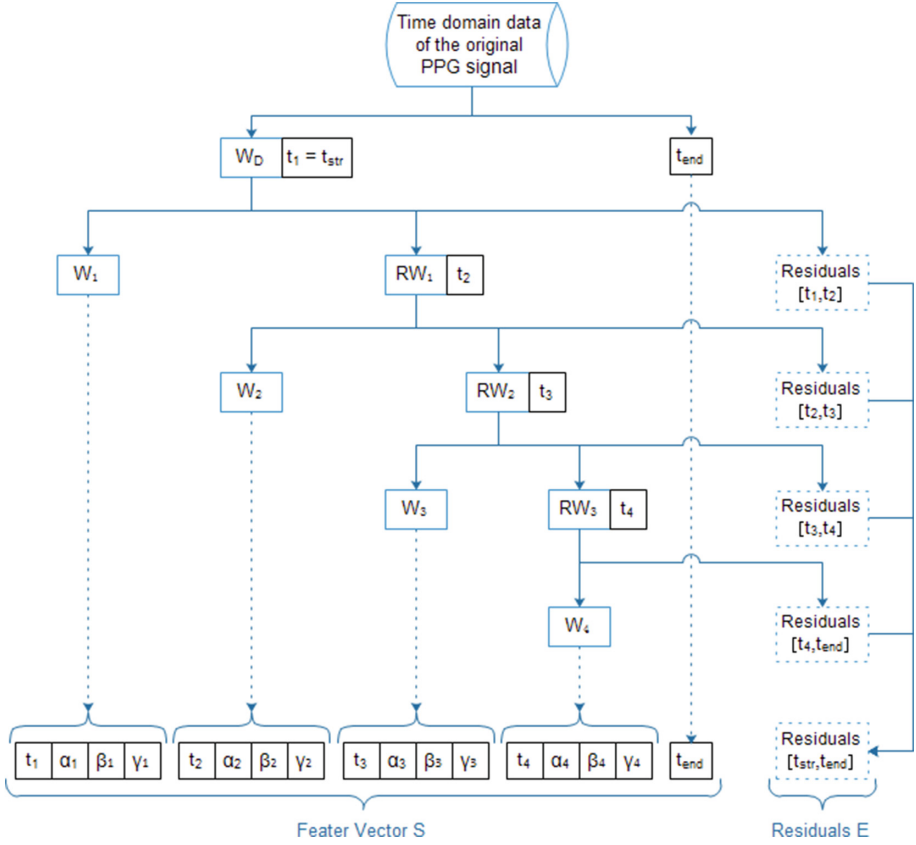


Fig. 2. The whole fitting process

$$t_1 = t_{str} \quad (4)$$

$$\begin{aligned} M_1 &= \exp(\beta_1 + \gamma_1/2), \quad t_{sd1} \leq M_1 \leq t_{p1} \\ \Rightarrow \ln(t_{sd1}) - \gamma_1/2 &\leq \beta_1 \leq \ln(t_{p1}) - \gamma_1/2 \end{aligned} \quad (5)$$

$$MSE_1 = \frac{1}{M_1} \sum_{t=t_1}^{t_1+M_1} (W_1(t) - W_D(t))^2, \quad t_1 \leq t \leq t_1 + M_1 \quad (6)$$

(b) Tidal Wave Fitting. RW_1 denotes the residual wave of W_D after the main wave fitting. The first peak of RW_1 is denoted as t_{p2} . t_{sd2} denotes the left zero crossing point around t_{p2} . M_2 represents the mode of W_2 . M_2 and its rang are expressed in Eq. (9). The time domain of Eq. (6) is between t_1 and $(t_1 + M_1)$. So the start time of W_2 denoted as t_2 equals $(t_1 + M_1)$. The optimal Lognormal basis representation is obtained by minimizing the mean squared error (MSE_2) between W_2 and RW_1 .

$$RW_1 = W_D - W_1 \quad (7)$$

$$t_2 = t_1 + M_1 \quad (8)$$

$$\begin{aligned} M_2 &= \exp(\beta_2 + \gamma_2/2), \quad t_{sd2} \leq M_2 \leq t_{p2} \\ \Rightarrow \ln(t_{sd2}) - \gamma_2/2 &\leq \beta_2 \leq \ln(t_{p2}) - \gamma_2/2 \end{aligned} \quad (9)$$

$$MSE_2 = \frac{1}{M_2} \sum_{t=t_2}^{t_2+M_2} (W_2(t) - RW_1(t))^2, \quad t_2 \leq t \leq t_2 + M_2 \quad (10)$$

(c) Dicrotic Wave Fitting. RW_2 denotes the residual wave of RW_1 after the tidal wave fitting. The first peak of RW_2 is denoted as t_{p3} . t_{sd3} denotes the left zero crossing point around t_{p3} . M_3 represents the mode of W_3 . M_3 and its rang are expressed in Eq. (13). The time domain of Eq. (10) is between t_2 and $(t_2 + M_2)$, so the start time of W_2 denoted as t_3 equals $(t_2 + M_2)$. The optimal Lognormal basis representation is obtained by minimizing the mean squared error (MSE_3) between W_3 and RW_2 .

$$RW_2 = RW_1 - W_2 \quad (11)$$

$$t_3 = t_2 + M_2 \quad (12)$$

$$\begin{aligned} M_3 &= \exp(\beta_3 + \gamma_3/2), \quad t_{sd3} \leq M_3 < t_{p3} \\ \Rightarrow \ln(t_{sd3}) - \gamma_3/2 &\leq \beta_3 < \ln(t_{p3}) - \gamma_3/2 \end{aligned} \quad (13)$$

$$MSE_3 = \frac{1}{M_3} \sum_{t=t_3}^{t_3+M_3} (W_3(t) - RW_2(t))^2, \quad t_3 \leq t \leq t_3 + M_3 \quad (14)$$

(d) Tail Wave Fitting. RW_3 denotes the residual wave of RW_2 after the dicrotic wave fitting. The time domain of Eq. (14) is between t_3 and $(t_3 + M_3)$, so the start time of W_4 denoted as t_4 equals $(t_3 + M_3)$. The end time of the fitting calculation here equals the end time of W_D denoted as t_{end} . The optimal Lognormal basis representation is obtained by minimizing the mean squared error (MSE_4) between W_4 and RW_3 .

$$RW_3 = RW_2 - W_3 \quad (15)$$

$$t_4 = t_3 + M_3 \quad (16)$$

$$MSE_4 = \frac{1}{t_{end} - t_4} \sum_{t=t_4}^{t_{end}} (W_4(t) - RW_3(t))^2, \quad t_4 \leq t \leq t_{end} \quad (17)$$

3 Simulation Results

The MIMIC II (Multiparameter Intelligent Monitoring in Intensive Care) Databases contain clinical signals and vital signs time series obtained from hospital medical information systems. The signals in the MIMIC II Databases are multiparameter recordings, which are obtained from both a bedside monitor and the medical records of the patient [14].

In this paper, a hundred individual records are extracted for simulations. The successive-fitting results are shown in Fig. 3.

As illustrated in Fig. 3, the four fitting processes all have a good fitting accuracy. The overall fitting result is shown in Fig. 4.

Table 1 shows the comparison results between the existing modeling methods and the proposed method. As showed in Table 1, the Lognormal methods has a much higher fitting accuracy than the Gaussian methods, this is because of the consistent long-tail feature between the Lognormal basis and the PPG pulse waveforms. And the number of the successive methods' per-fitting parameters is far less than the single methods'. So, for these Lognormal methods, although the single fitting method is a little bit better than the proposed method in fitting accuracy, it performed poorly in

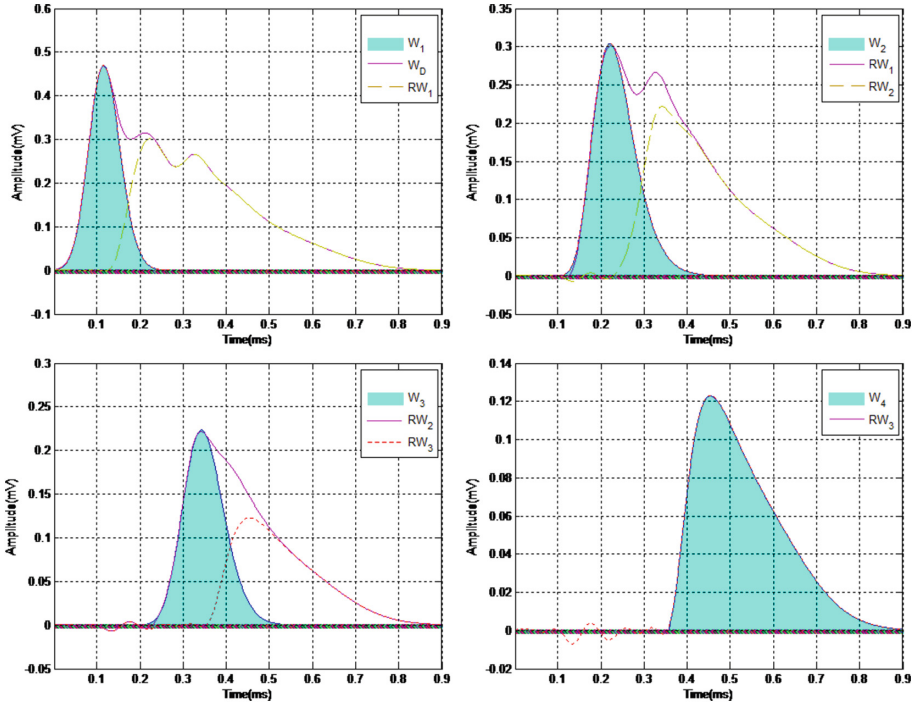


Fig. 3. Successive-fitting results

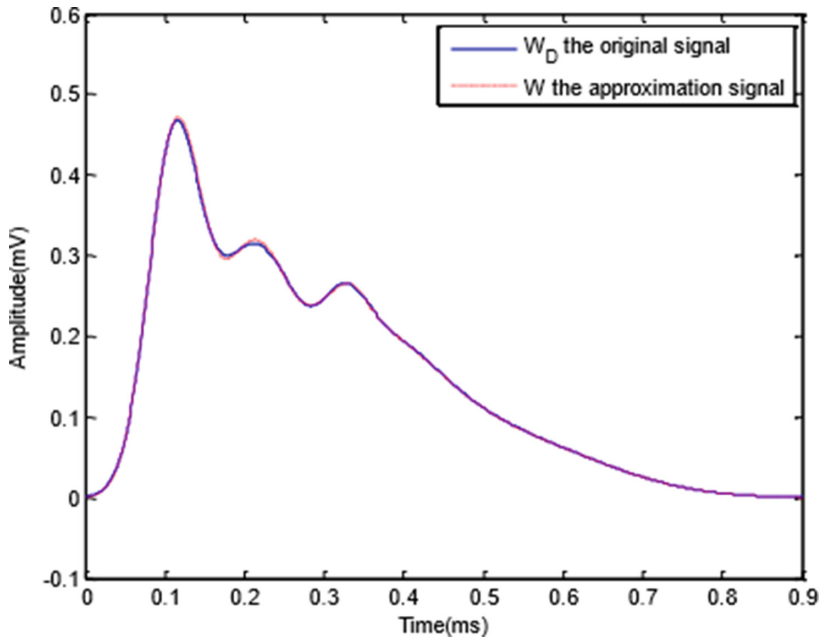


Fig. 4. Overall fitting result

Table 1. Fitting accuracy of several different models of PPG signal

Bases type	Gaussian	Gaussian	Gaussian	Lognormal	Lognormal	Lognormal
Bases no.	2	3	4	4	4	4
Fitting type	Single				Successive	
					Fixed time domain	Adaptive time domain
Parameters no. per fitting	6	9	12	16	4	4
Average MSE	0.2073	0.1792	0.1508	0.0165	0.0192	0.0171

terms of fitting efficiency. And for the successive lognormal methods, as showed in Table 1, the proposed method has better performance on fitting accuracy than the one with fixed time domain. The results have proved that the proposed method can meet the requirements of both accuracy and efficiency for daily monitoring of cardiovascular health.

4 Conclusion

PPG signal carries abundant physiological and pathological information of cardiovascular system, which can be used for daily monitoring of cardiovascular health in BSNs. The simulation results show that, compared with the existing methods, the modeling method based on the long-tail Lognormal basis not only has a high fitting accuracy, but also has good computational complexity, thus being more suitable for the real time application to daily cardiovascular health monitor in the BSNs.

Acknowledgement. This paper is supported in part by the National Natural Science Foundation of China (61571336), the International science & technology cooperation project (No. 2015DFG12210).

References

1. Fortino, G., Giannantonio, R., Gravina, R., et al.: Enabling effective programming and flexible management of efficient body sensor network applications. *IEEE Trans. Human-Machine Syst.* **43**(1), 115–133 (2013)
2. Fortino, G., Giampà, V.: PPG-based methods for non invasive and continuous blood pressure measurement: an overview and development issues in body sensor networks. In: *IEEE International Workshop on Medical Measurements and Applications Proceedings*, pp. 10–13 (2010)
3. Chen, W., Lei, S., Guo, L., Chen, Y., Pan, M.: Study on conditioning and feature extraction algorithm of photoplethysmography signal for physiological parameters detection. In: *Proceedings of the Image and Signal Processing*, pp. 15–17 (2011)
4. Allen, J.: Photoplethysmography and its application in clinical physiological measurement. *Physiol. Meas.* **28**(3), 1–39 (2007)
5. Kyriacou, P.A., Powell, S., Langford, R.M., Jones, D.P.: Investigation of oesophageal photoplethysmographic signals and blood oxygen saturation measurements in cardiothoracic surgery patients. *Physiol. Meas.* **23**(8), 533–545 (2002)
6. Johansson, A.: Neural network for photoplethysmographic respiratory rate monitoring. *Med. Biol. Eng. Comput.* **41**(5), 242–248 (2003)
7. Binns, S.H., Sisson, D.D., Buoscio, D.A., Schaeffer, D.J.: Doppler ultrasonographic, oscillometric sphygmomanometric, and photoplethysmographic techniques for noninvasive blood-pressure measurement in anesthetized cats. *J. Vet. Intern. Med.* **9**(6), 405–414 (1995)
8. Li, D., Zhao, H., Li, S., Zheng, H.: A new representation of photoplethysmography signal. In: Cai, Z., Wang, C., Cheng, S., Wang, H., Gao, H. (eds.) *WASA 2014. LNCS*, vol. 8491, pp. 279–289. Springer, Heidelberg (2014)
9. Martin-Martinez, D., Casaseca-de-la-Higuera, P., Martin-Fernandez, M., et al.: Stochastic modeling of the PPG signal: a synthesis-by-analysis approach with applications. *IEEE Trans. Biomed. Eng.* **60**(9), 2432–2441 (2013)
10. He, X., Goubran, R.A., Liu, X.P.: Secondary peak detection of PPG signal for continuous cuffless arterial blood pressure measurement. *IEEE Trans. Instrum. Measur.* **63**(6), 1431–1439 (2014)
11. Huotari, M., Vehkaoja, A., Määtä, K., et al.: Photoplethysmography and its detailed pulse waveform analysis for arterial stiffness. *J. Struct. Mech.* **44**(4), 345–362 (2011)

12. Kostamovaara, J.: Arterial stiffness estimation based photoplethysmographic pulse wave analysis. In: Proceedings of the Spie, pp. 73–76 (2010)
13. Zhao, H., Dou, S.C., Li, D.Z., et al.: Mathematical modeling of pulse wave based on lognormal function. J. Northeast. Univ. Nat. Sci. **37**(2), 169–173 (2016)
14. Database of MIMIC II (2016). <http://physionet.org/mimic2/mimic2&underscore;waveform&underscore;overview.shtml>

Internet and Distributed Computing Systems

9th International Conference, IDCS 2016, Wuhan,

China, September 28-30, 2016, Proceedings

Li, W.; Ali, S.; Lodewijks, G.; Fortino, G.; Di Fatta, G.; Yin,

Z.; Pathan, M.; Guerrieri, A.; Wang, Q. (Eds.)

2016, XV, 526 p. 226 illus., Softcover

ISBN: 978-3-319-45939-4